# Evidence of dark solitons in all-normal-dispersion-fiber lasers

D. Y. Tang,[1,2,*] L. Li,[2] Y. F. Song,[2] L. M. Zhao,[1] H. Zhang,[3] and D. Y. Shen[1]
[1]*School of Physics and Electronic Engineering, Jiangsu Normal University, Xuzhou 221116, China*
[2]*School of Electrical and Electronic Engineering, Nanyang Technological University, Singapore 639798*
[3]*College of Physics and Microelectronic Science, Hunan University, Changsha 410082, China*
(Received 8 December 2012; revised manuscript received 15 April 2013; published 29 July 2013)

In a recent paper we reported dark pulse emission of an all-normal-dispersion-fiber laser [Zhang, Tang, Zhao, and Wu, Phys. Rev. A **80**, 045803 (2009)]. However, the formation mechanism of the dark pulse in the laser was unclear due to the limited temporal resolution of the measurement system. Using an improved detection system we have further investigated the phenomenon. We not only experimentally, unambiguously confirmed the existence of dark solitons in the fiber laser, but also identified that the dark pulses observed previously were bunches of the dark solitons. Moreover, we show that the dark soliton formation is a generic feature of the all-normal-dispersion-fiber lasers.

DOI: 10.1103/PhysRevA.88.013849 PACS number(s): 42.65.Tg, 42.65.Re, 42.55.Wd, 42.65.Sf

## I. INTRODUCTION

In a recent paper [1] we reported the experimental observation of a type of dark pulse emission in an erbium-doped fiber ring laser made of all-normal-dispersion fibers. The fiber laser has a cavity configuration that is similar to that of the conventional passively mode-locked fiber lasers with the nonlinear polarization rotation technique [2]. It is well known that for a fiber laser with such a cavity configuration there are two linear cavity phase bias regimes of the laser operation [3]. In one regime the nonlinear phase shift of light will lead to the generation of an artificial saturable absorber effect of the cavity (positive cavity feedback), and consequently the self-started mode locking of the laser could occur. In another regime the nonlinear phase shift of light generates an antisaturable absorber effect of the cavity (negative cavity feedback), where no mode locking of the laser is possible. We found experimentally that by operating an all-normal-dispersion-cavity-fiber laser in the latter linear cavity phase bias regime, under appropriate laser operation conditions, a stable train of dark pulses with the cavity fundamental repetition rate could be formed in the laser. Based on the nonlinear Schrödinger equation (NLSE) that describes the nonlinear light propagation in the single-mode fibers (SMFs), bright solitons are formed in the anomalous-dispersion SMFs, and dark solitons are formed in the normal-dispersion SMFs. Therefore, the formation of the stable dark pulses in the fiber laser was explained as a result of the dark soliton shaping. Indeed, under the dark pulse emission the optical spectrum of the laser emission also became broader than the stable cw emission. Based on the spectrum broadening and assuming that the formed dark solitons have a transform-limited hyperbolic-tangent profile, it was estimated that if a dark soliton would have been formed in the fiber laser, the formed dark solitons would have a pulse width of several picoseconds [1]. Later in a comment on the paper by Coen and Sylvestre [4], it was pointed out that the experimentally observed dark pulses could not be the dark solitons formed in the fiber laser. Because in the experiment an electronic detection system with a bandwidth of 1 GHz was used, if the formed dark solitons had only a several-picosecond pulse width, they would not have been detectable by the detection system. Hence the experimentally observed dark pulses with a near 100% darkness should have a much broader pulse width. Coen and Sylvestre's comment is obviously correct. However, if the observed dark pulses were not the dark solitons formed in the fiber laser, then why did the laser emission have a broad optical spectrum? What is the relation between the broad dark pulses and the broadened optical spectrum? Was there dark soliton formation in the fiber laser? All these are the pressing questions that need to be answered.

The key to the questions is to find a way to measure in real time the narrow dark pulses formed in the laser. However, differently from the bright solitons, whose existence in a laser could be easily identified even with a moderate-speed photodetector and oscilloscope, it is unfortunately not so straightforward to detect a dark soliton formed in a laser. This probably is the main reason that so far no experimental observation on the individual dark soliton in fiber lasers has been reported. Thanks to the rapid advance of the ultrafast optoelectronics technology, we are now in the position to use ultrahigh-speed real-time electronic detection systems to directly measure narrow dark pulses. Using an ultrahigh-speed detection system with a temporal resolution of 30 ps we have further experimentally investigated the dark pulse emission of our fiber laser. In this paper we present our experimental results. We not only show clear experimental evidence of the existence of dark solitons in the all-normal-dispersion-cavity-fiber lasers, but also show that the dark soliton formation is an intrinsic feature of the lasers.

## II. EXPERIMENTAL SETUP AND RESULTS

For our current experiment an all-normal-dispersion-cavity erbium-doped fiber laser with a cavity configuration as reported previously [1] was constructed. To demonstrate that the observed dark pulse emission is a general feature of all-normal-cavity-dispersion-fiber lasers whose occurrence is independent of the detailed cavity parameters, we used a piece of 3-m erbium-doped fiber (EDF) that has an erbium-doping concentration of 2880 ppm and a value of group velocity dispersion (GVD) of $-32$ (ps/nm)/km as the gain medium of the laser, and made the total cavity an arbitrary length of

*Corresponding author: edytang@ntu.edu.sg

 

10.5 m. The rest of the cavity fibers used were the dispersion compensation fiber (DCF) that has a GVD of −4 (ps/nm)/km. Again a high-power Fiber Raman Laser (KPS-BT2-RFL-1480-60-FA) at a wavelength of 1480 nm was used as the pump source. The pump light was coupled to the fiber cavity through a wavelength division multiplexer (WDM), and a 10% fiber coupler was used to output the laser emission. All the intracavity components (WDM, output coupler, and isolator) were either specially made with the DCF or pigtailed with it. The total cavity dispersion was estimated as about ∼0.167 $ps^2$. An optical spectrum analyzer (Ando AQ-6315B), and a high-speed oscilloscope (DSA-x 93204A 33GHz, Agilent Technologies) together with two 45-GHz photodetectors (Newfocus Model 1014) were used to monitor the laser output.

A major improvement of the current experiment from that reported previously is that an ultrahigh-speed detection system was used to monitor the laser emission in real time. The detection system (photodetector and oscilloscope) has a temporal resolution as short as ∼30 ps. Tested with a femtosecond mode-locked fiber laser source, we also experimentally confirmed that the rising and falling time of the detection system is ∼12 ps. This detection system allows us to easily distinguish a picosecond-level dark pulse from the background noise. An external cavity-fiber-pigtailed polarization beam splitter (PBS) together with an external cavity polarization controller was used to resolve the two orthogonal polarization components of the laser emission. Therefore, based on the measured results we could also determine if the dark pulses obtained are linearly polarized or not.

We first repeated the previous experiment and confirmed that all the dark pulse emission features reported were reproducible in the current laser. Figure 1 shows, for example, the single dark pulse emission of the laser measured with a 1-GHz bandwidth detection system and the high-speed detection system, respectively. Measured with a 1-GHz detection bandwidth a nice stable dark pulse train with the fundamental cavity repetition rate was obtained. When measured with the high-speed detection system the dark pulse train was still visible on the oscilloscope trace; however, the cw background then displayed large-amplitude, high-frequency-noise-like intensity modulations. Confirmed by the high-speed measurement the dark pulses indeed have a subnanosecond pulse width.

To determine the formation mechanism of the observed broad dark pulses, we then experimentally investigated the variation of laser emission with the pump power increase. A generic evolution observed is shown in Fig. 2. At a relatively low pump power (∼68 mW), the fiber laser emitted a weak continuous wave (cw), as shown in Fig. 2(a). In this state the measured oscilloscope trace is stable. We note that in each of the plots in Fig. 2 two oscilloscope traces corresponding to each of the two orthogonal polarization components of the laser emission are displayed. As the emission of the fiber laser was actually linearly polarized, one trace always has, therefore, zero intensity. The zero intensity trace serves here as a reference to indicate the actual noise level of the detection system. Figure 3 shows the optical spectra of the laser emissions. The center wavelength of the laser emission was at 1577.4 nm. In the stable cw laser emission the optical spectrum was a narrow line with a 3-dB bandwidth of ∼0.07 nm. As the pump power was increased to ∼100 mW, the oscilloscope

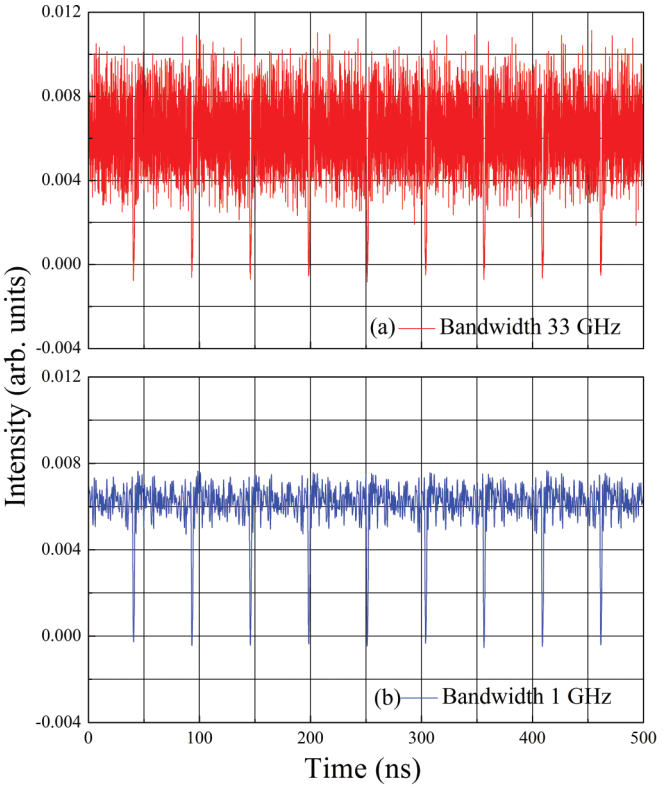


FIG. 1. (Color online) A train of the dark pulse emission of the fiber laser. Upper trace: laser emission measured with 33-GHz detection bandwidth; lower trace: laser emisison measured with 1-GHz detection bandwidth.

trace, then gradually became unstable. Narrow dark pulses also appeared obviously on the oscilloscope trace, as shown in Fig. 2(b). As the pump power was further increased, more and more dark pulses appeared on the oscilloscope trace, as shown in Fig. 2(c). Associated with the appearance of the dark pulses, the optical spectrum of the laser emission also became broader. A typical spectrum measured at 400 mW pumping power is shown in Fig. 3; its 3-dB bandwidth is ∼0.2 nm. To highlight the features of the dark pulses, in Fig. 4(a) we have zoomed in on a segment of the oscilloscope trace. Within a time interval of ∼600 ps, there were five dark pulses. The durations of the dark pulses on the oscilloscope trace were ∼30 ps, which is the limitation of the detection system. Therefore, the real dark pulse width could be even narrower than that. Based on the 3-dB spectral bandwidth of the laser emission and assuming that the dark pulses have a transform-limited hyperbolic-tangent profile, we estimated that the width of the dark pulses should be ∼13 ps. At the pump power of 400 mW the laser output power was ∼9.6 mW. Considering that the average cavity dispersion of $\beta_2$ is ∼15.9 $ps^2$/km, assuming that a black soliton was formed and the nonlinear fiber coefficient $\gamma = 3\ W^{-1}\ km^{-1}$, based on the soliton formation $P_0 = \frac{\beta_2}{\gamma\tau^2}$ the estimated soliton pulse width would be 13.1 ps. Therefore, we believe that the dark pulses on the oscilloscope trace should be the dark solitons formed in the fiber laser.

We had also experimentally studied the filter effects of the detection system on the measured results. As displayed in Fig. 4(b), by changing the bandwidth of the detection system to 5 and 10 GHz, the measured intensity dips would become

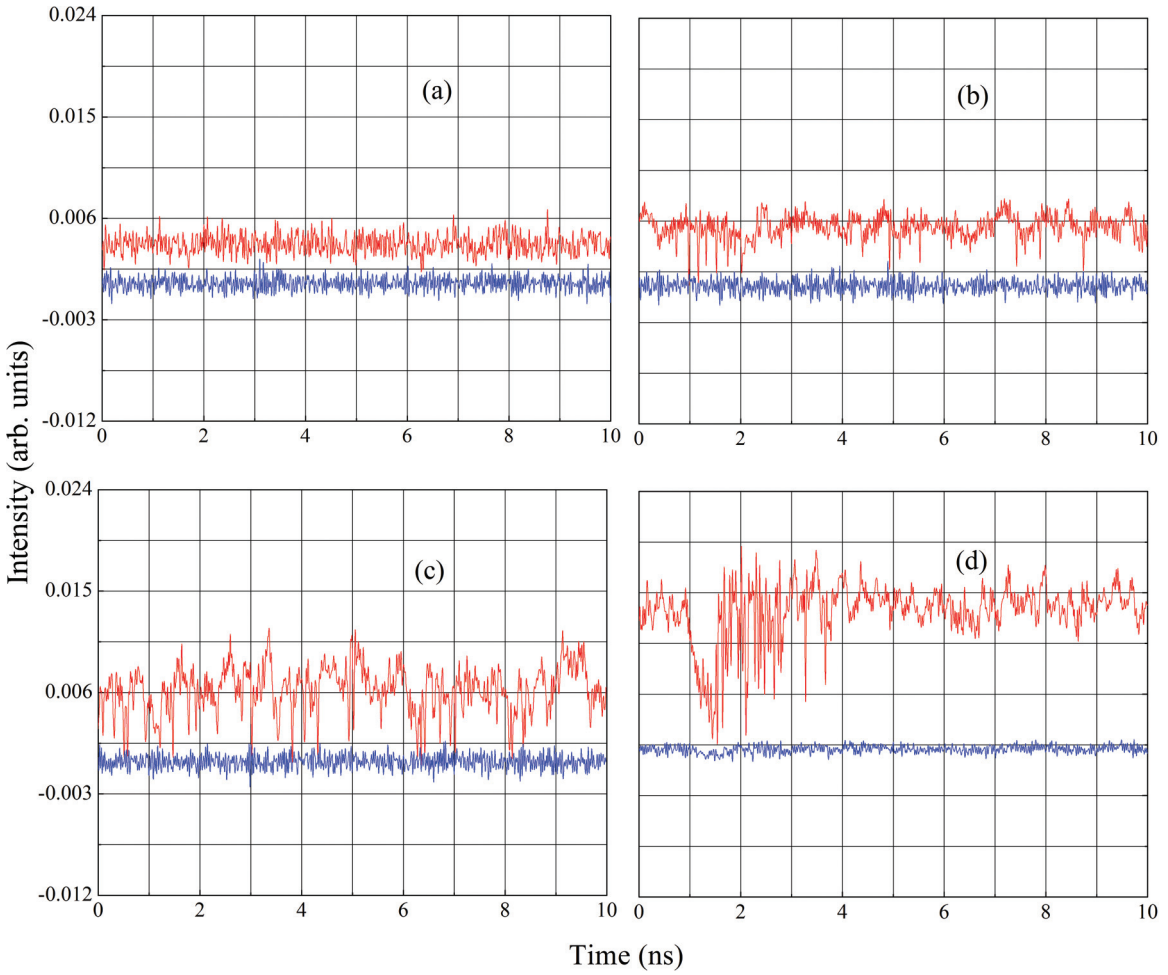


FIG. 2. (Color online) Oscillscope traces of the laser emission under different pump power. (a) ∼68 mW, (b) ∼100 mW, (c) ∼400 mW, (d) ∼700 mW. Upper trace: laser emission. Lower trace: reference signal showing system noise level.

broader and much shallower. Hence, despite the existence of the dark solitons in the fiber lasers, if measured with a narrow-bandwidth detection system the dark solitons would not be detectable.

As shown in Figs. 2(b) and 2(c) the dark solitons are randomly distributed in the whole cavity, and the stronger the pump strength, the denser the dark solitons. However, an interesting effect was observed experimentally that above a certain strong pump level—in our experiment this was about ∼700 mW—the dark solitons always automatically bunched together, as shown in Fig. 2(d). As a result of the dark soliton bunching a broad dark pulse was then formed in the cavity; e.g., on the oscilloscope trace shown in Fig. 2(d) a broad dark pulse with a pulse width of 450 ps was formed, and immediately after the broad dark pulse there were many dark solitons approaching it. We had experimentally measured the state with a 1-GHz bandwidth detection system and confirmed that the soliton bunching was displayed as a nanosecond-level dark pulse. The experimental result clearly explained how the broad dark pulses reported previously were formed. We note that formation of bound states of solitons and soliton bunching is a well-known feature of the bright solitons formed in fiber lasers [5,6]. Our experimental result shows that, like the bright solitons, the dark solitons formed in a fiber laser also have the tendency of bunching.

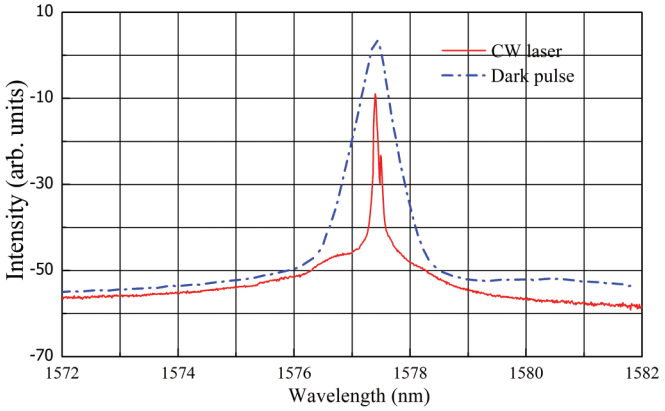


FIG. 3. (Color online) Optical spectra of the laser under cw and dark pulse emissions.

## III. NUMERICAL SIMULATIONS

To confirm that dark solitons could be formed in our fiber laser—in particular, the formed dark solitons have comparable soliton parameters to those observed experimentally—we

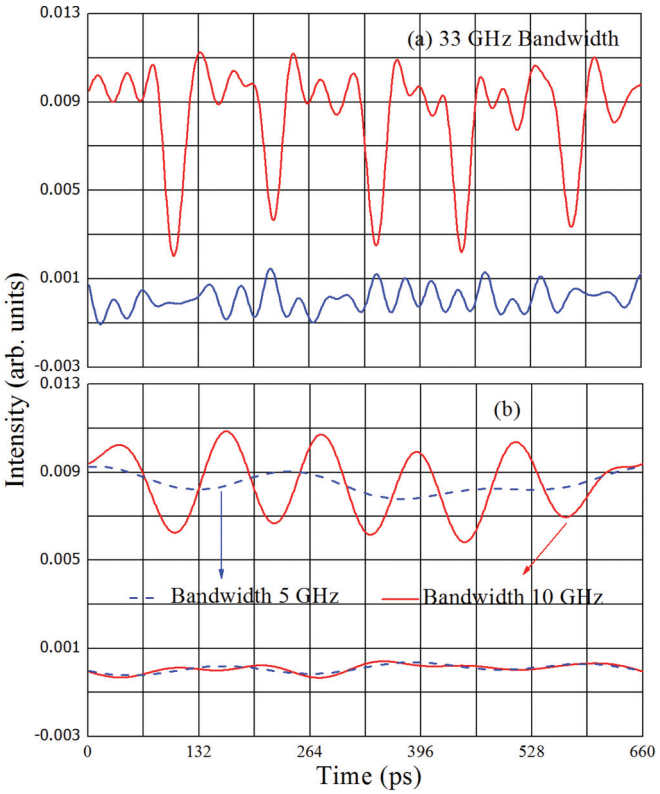


FIG. 4. (Color online) Zoom-in of the laser emission. (a) Oscilloscope trace measured with 33-GHz bandwidth. (b) Oscilloscope traces measured with 5- and 10-GHz bandwidth. Upper trace: laser emission. Lower trace: reference signal showing system noise level.

further numerically simulated the laser operation under the experimental conditions. We used exactly the same model as reported in [3] to simulate the operation of the fiber laser. It has been shown previously that the model could faithfully reproduce the various features of the bright solitons experimentally observed in the passively mode-locked fiber lasers with the nonlinear polarization rotation technique [3]. Although under the dark soliton emission the laser is no longer operating in the mode-locking regime, we note that the basic properties of the nonlinear light propagation in the cavity are still the same. Hence, the same model can also be used to simulate the dark soliton operation of the fiber laser.

We used the following coupled extended Ginzburg-Landau equations to describe the nonlinear light propagation in the cavity fibers:

$$\frac{\partial u}{\partial z} = i\beta u - \delta\frac{\partial u}{\partial t} - \frac{ik''}{2}\frac{\partial^2 u}{\partial t^2} + \frac{k'''}{6}\frac{\partial^3 u}{\partial t^3} + i\gamma\left(|u|^2 + \frac{2}{3}|v|^2\right)u + \frac{i\gamma}{3}v^2u^* + \frac{G}{2}u + \frac{G}{2\Omega_g^2}\frac{\partial^2 u}{\partial t^2},$$
$$\frac{\partial v}{\partial z} = -i\beta v + \delta\frac{\partial v}{\partial t} - \frac{ik''}{2}\frac{\partial^2 v}{\partial t^2} + \frac{k'''}{6}\frac{\partial^3 v}{\partial t^3} + i\gamma\left(|v|^2 + \frac{2}{3}|u|^2\right)v + \frac{i\gamma}{3}u^2v^* + \frac{G}{2}v + \frac{G}{2\Omega_g^2}\frac{\partial^2 v}{\partial t^2}, \quad (1)$$

where $u$ and $v$ are the normalized envelopes of the light along the two orthogonal polarization axes of the fiber. $2\beta = 2\pi\Delta n/\lambda$ is the wave-number difference between the two polarization modes. $2\delta = 2\beta\lambda/2\pi c$ is the inverse group velocity difference. $k''$ is the second-order dispersion coefficient, $k'''$ is the third-order dispersion coefficient, and $\gamma$ represents the nonlinearity of the fiber. $G$ is the saturable gain coefficient of the fiber. For the undoped fiber $G = 0$, and for the erbium-doped fiber we further considered the gain saturation as

$$G = G_0 \exp\left[-\frac{\int(|u|^2 + |v|^2)dt}{E_{\text{sat}}}\right],$$

where $G_0$ is the small signal gain coefficient, and $E_{\text{sat}}$ is the normalized saturation energy.

To also take into account the actions of the various cavity components such as the polarizer and output coupler on the light, we used the so-called pulse tracing method for the simulation. Briefly, we monitored a small segment of the light field within the laser cavity. Starting the simulation with a weak cw light that has a small dip on top of it, we let the light circulate in the cavity. When the light encounters a cavity component, we multiply the Jones matrix of the component to the light field. After one cavity round trip we then used the result of the previous round calculation as the input of the next round calculation. The process was repeated until a stable field was obtained. With this technique not only the nonlinear light propagation effects in the cavity fiber but also the cavity feedback and cavity boundary condition were automatically considered.

To make the simulations as close as possible to the experimental situation, we used the following parameters for our simulations: nonlinear fiber coefficient $\gamma = 3\ \text{W}^{-1}\,\text{km}^{-1}$; erbium fiber gain bandwidth $\Omega_g = 16$ nm; fiber dispersions $D''_{\text{EDF}} = -32$ (ps/nm)/km, $D''_{\text{DCF}} = -4$ (ps/nm)/km, and $D''' = 0.01$ (ps$^2$/nm)/km; cavity length $L = 3.0\ \text{m}_{\text{EDF}} + 6.5\ \text{m}_{\text{DCF}} = 9.5$ m; cavity birefringence $L/L_b = 9.5/100$ and the nonlinear gain saturation energy $E_{\text{sat}} = 480$ pJ. As in the experiment we used the laser gain coefficient and the cavity linear phase delay bias as the control parameters.

Independent of the concrete cavity parameters, as far as the linear cavity phase delay bias was set in the no-mode-locking regime, stable dark solitons could always be obtained in our simulations. With a cavity linear phase delay bias setting of $0.9\pi$ and the gain coefficient of $G_0 = 1100\ \text{km}^{-1}$, a typical stable dark soliton numerically calculated is shown in Fig. 5. Figure 5(a) shows that with the cavity round trips, the dark pulse is stable, suggesting that it is a dark soliton of the laser. Figure 5(b) shows the calculated pulse intensity profile. By fitting the pulse intensity profile with that of a standard dark soliton, the dark pulse has a duration of about 11.5 ps, which is comparable with that estimated from the experimentally measured soliton spectrum. Figure 5(c) is the corresponding calculated dark soliton spectrum. The calculated soliton spectrum also has a sharp narrow peak, which is similar to the experimental result. No spectral sidebands are observable on the soliton spectrum as the formed dark soliton has a broad pulse width and the cavity has a short length of 9.5 m. Depending on the laser gain

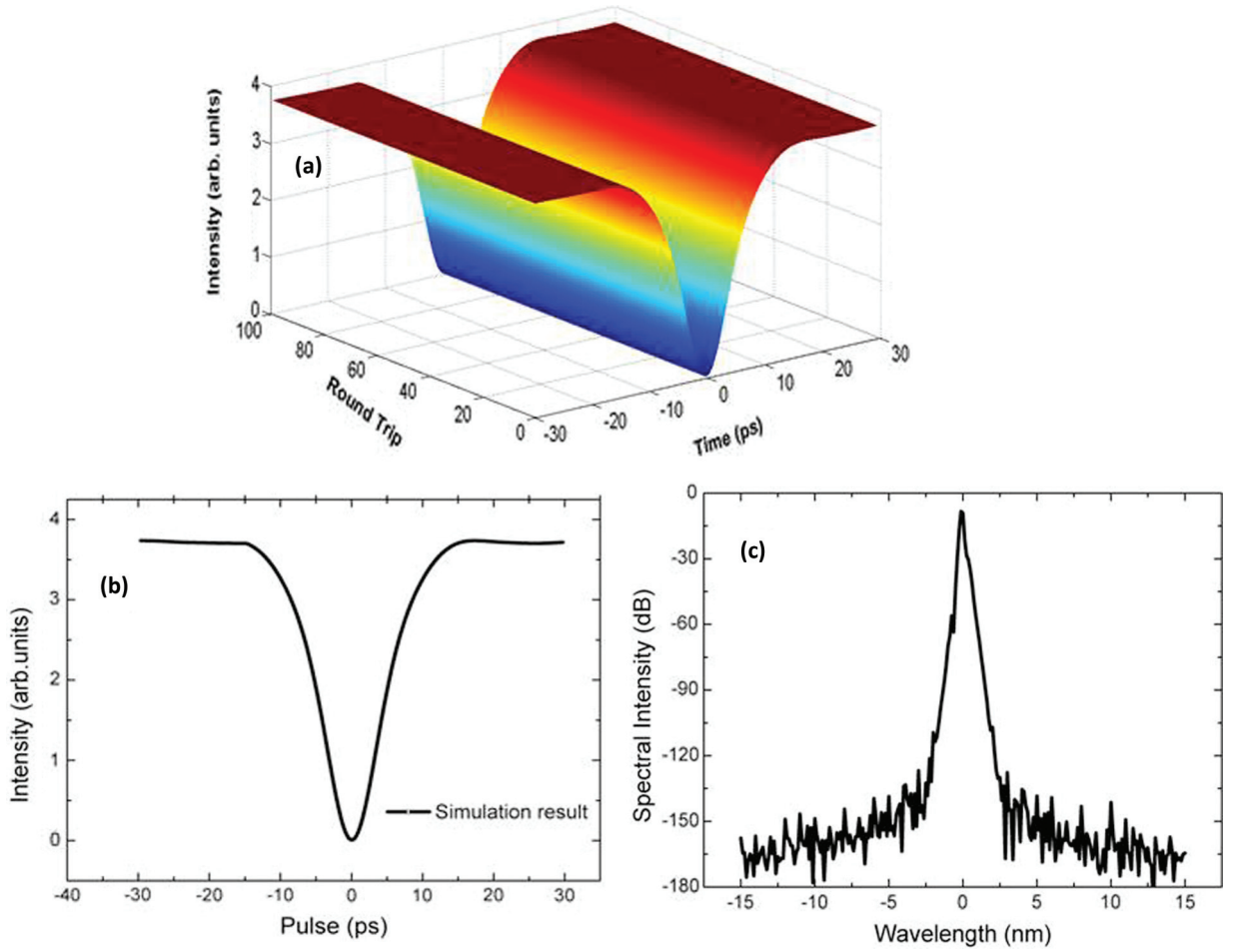


FIG. 5. (Color online) A typical state of the dark soliton operation of the fiber laser numerically calculated. (a) The evolution of the dark soliton with the cavity round trips; (b) the soliton pulse profile; (c) the corresponding soliton spectrum.

and gain saturation energy settings, numerically gray solitons with different darkness were also obtained. Associated with the different darkness of the gray solitons the pulse width also varied. Coexistence of multiple black solitons, and black and gray solitons in the same cavity were also numerically obtained. Under suitable conditions the black and gray solitons could also form a soliton bunch and propagate as a unit in the cavity. Our numerical simulations have well reproduced the experimental results and explained why no energy quantization was observed for the dark solitons in the experiments.

## IV. DISCUSSIONS

Differently from the bright solitons formed in the mode-locked fiber lasers, where one can effectively control the number of solitons in the cavity through carefully controlling the pump strength, it was found experimentally that it is almost impossible to control the number of the dark solitons. To understand the feature of the dark solitons we note that Gredeskul and Kivshar have theoretically shown that different from the NLSE type of bright solitons, whose formation requires a certain fixed pulse intensity threshold, the formation of the NLSE type of dark solitons has no threshold [7]. Any small initial intensity dip could be evolved into dark solitons. Our experimental result well confirmed the theoretical prediction. All the dark solitons were automatically formed in the cavity once the intracavity laser intensity became sufficiently strong, which is different from the bright soliton formation in a fiber laser, where in order to form the bright solitons a mode-locked pulse needs to be formed *a priori*. As the dark solitons can be easily formed—and in a fiber ring laser there are plenty of sources, e.g., the environmental noise and the mode beating, that could cause weak intensity dips—many dark solitons were simultaneously formed in the laser cavity. The dark solitons are randomly embedded in the laser emission. However, due to their narrow pulse width they are undetectable with even a moderate (<15 GHz) speed detection system. Only under sufficiently strong pumping where the dark solitons have bunched together and formed a giant dark pulse, their existence would then become detectable with even 1-GHz bandwidth detection systems as reported previously [1]. Physically, a dark soliton is equivalent to a bright soliton reversely embedded in a cw intensity background. Hence, dark solitons also have a broad optical spectrum. Once a dark soliton is formed in a laser, the spectral bandwidth of the laser emission will therefore always become broader than the cw emission. The narrower the formed dark soliton pulses, the broader the laser emission spectrum. Finally, we note that the broad dark pulses formed under strong pump power in our laser are actually bunches of dark solitons. The width of the "dark pulses" is determined

by the number of the dark solitons within a bunch. So far we have not understood why under high pump power the dark solitons always bunch together. However, considering that under strong pumping the negative cavity feedback of the laser also becomes strong, and under strong positive cavity feedback the bright solitons formed in a mode-locked fiber laser have the tendency of bunching together, it might be understandable that under action of strong negative cavity feedback, the dark solitons would also bunch together.

## V. CONCLUSION

In conclusion, we have experimentally investigated the dark pulse emission of an all-normal-dispersion-fiber laser by using an ultrahigh-speed detection system. Based on the real-time monitoring on the laser emission, we confirmed the NLSE-type dark soliton formation in the fiber laser. Especially, our experimental results have shown that the dark soliton formation is an intrinsic feature of the fiber lasers. As the dark soliton formation has no threshold, many dark solitons are always formed in a laser. However, their existence could not be easily detected if a moderate bandwidth detection system is used, except that the dark solitons are bunched together to form a giant dark pulse.

## ACKNOWLEDGMENTS

The project is partially supported by the funds of Priority Academic Program Development of Jiangsu Higher Education Institutions (PAPD), China, Minister of Education (MOE) Singapore, under Grant No. 35/12, and AOARD under Agreement No. FA2386-13-1-4096.

[1] H. Zhang, D. Y. Tang, L. M. Zhao, and X. Wu, Phys. Rev. A **80**, 045803 (2009).
[2] V. J. Matsas, T. P. Newson, D. J. Richardson, and D. N. Payne, Electron. Lett. **28**, 1393 (1992).
[3] D. Y. Tang, L. M. Zhao, B. Zhao, and A. Q. Liu, Phys. Rev. A **72**, 043816 (2005).
[4] S. Coen and T. Sylvestre, Phys. Rev. A **82**, 047801 (2010).
[5] D. Y. Tang, B. Zhao, L. M. Zhao, and H. Y. Tam, Phys. Rev. E **72**, 016616 (2005).
[6] S. Chouli and P. Grelu, Opt. Exp. **17**, 11776 (2009).
[7] S. A. Gredeskul and Y. S. Kivshar, Phys. Rev. Lett. **62**, 977 (1989).